JACS
JOURNAL OF THE AMERICAN CHEMICAL SOCIETY

Communication

pubs.acs.org/JACS

Self-Adjustable Crystalline Inorganic Nanocoils

Peng-peng Wang, Yong Yang, Jing Zhuang, and Xun Wang*

Department of Chemistry, Tsinghua University, Beijing 100084, P. R. China

Supporting Information

ABSTRACT: Biomacromolecules such as proteins, although extremely complex in microstructure, can crystallize into macro-sized crystals after self-adjusting their shapes, based on which the structure of biology is built. Inorganic nanowires/nanoribbons with a similar one-dimensional topology but much simpler structures can hardly be as flexible as macromolecules when constructing superlattice structures because of their inherent rigidity. Here we report the synthesis of crystalline indium sulfide nanoribbon-based nanocoils that are formed by spontaneous self-coiling of ultrathin nanoribbons. The nanostructures are flexible and appear as relatively random coils because of their ultrathin ribbon structures (~0.9 nm in thickness) with high aspect ratios. Moreover, the nanocoils can self-adjust their shapes and assemble into two-dimensional superlattices and three-dimensional supercrystals in solution. The ultrathin nanocoils are expected to bring new insights into the use of flexible nanocrystals as building blocks for constructing superstructures.

Self-assembly of nanocrystals provides a powerful approach for constructing superlattices and supercrystals that are of great importance from both fundamental and applicative standpoints.[1−5] Of these assembly systems, inorganic nanoparticles with round, rod, wire, polyhedral, and other shapes[3−9] are usually regarded as "hard" building blocks because they can hardly change their shapes when assembling into ordered structures, which limits the complexity of the assembled structures and narrows the types of building blocks for understanding of crystallization to some extent. It is known that macromolecules, especially biological polymers such as proteins, are the most sophisticated building blocks available to an organism.[10,11] From a more realistic view of shapes, many of them are commonly visualized as random chains that can fold into well-behaved structures and then crystallize into macro-sized crystals.[12−15] Inspired by organic systems, we wondered whether we could obtain inorganic nanocrystal building blocks with a similar one-dimensional topology that can show shape flexibility and crystallize into superstructures.

One-dimensional inorganic nanostructures with high aspect ratios can be bent and shaped into complex architectures.[16−20] To date, ZnO nanorings[21] and helices[22] as well as carbon nanotube-based nanorings[20,23,24] formed by self-coiling or constrained coiling of their one-dimensional nanostructures have been reported. If their diameters/thicknesses were to shrink further to the subnanometer scale, it would be imaginable that inorganic nanowires/nanoribbons might be more flexible and to some extent could show chain bending, coiling,[17,19] and even crystallization behavior similar to that of flexible biomacromolecules. Furthermore, inorganic nanoparticles can also be treated as protein mimics because of their similarities in overall size and surfaces.[25] Here we report the synthesis of crystalline indium sulfide nanoribbon-based ultrathin nanocoils (UNCs) that are formed by spontaneous self-coiling of ultrathin nanoribbons as they grow in solution. Electron microscopy revealed that the as-synthesized nanoribbons are only ~0.9 nm in thickness and up to hundreds of nanometers in length. Because of their subnanometer-scale thickness, the UNCs are flexible and appear as relatively random coils. Notably, in remarkable contrast with those "hard" building blocks that have been the focus of particle assembly in the past, the UNCs have a strong tendency to self-adjust their shapes and assemble into supercrystals in solution in a manner analogous to macromolecule crystallization in which molecular chains fold together and form ordered structures.

The UNCs were synthesized via a simple solution-phase reaction. From sulfur powder and indium acetate as precursors and octylamine and ethanol as solvents, inorganic nanocoils with rich shape flexibility were easily obtained at 180−220 °C. The octylamine served not only as a solvent but also as a surface ligand. The N−H modes at 1650−1450 cm^{-1} and the CH_2 and CH_3 stretching vibrations at 2800−3000 cm^{-1} in the Fourier transform infrared (FT-IR) spectrum indicated that the products were capped with octylamine[26] [Figure S1 in the Supporting Information (SI)].

The shape of the product was determined by transmission electron microscopy (TEM) (Figure 1; enlarged images are shown in Figure S2). A low-magnification TEM image of the sample shows large areas of circular shapes of nanowires (Figure 1a), whereas a closer examination indicates that these coils are not made of nanowires but of ultrathin nanoribbons, as revealed by those loose coils exposing lateral surface (Figure 1b). This was further confirmed by a set of tilted TEM images of the nanocoils (Figure S3). Because of their ultrathin nanostructure (only ~0.9 nm in thickness), these UNCs can show flexible coiling shapes, such as double-headed coils with different loops and unclosed ringlike and S-shaped coils (Figure 1e). The high-resolution TEM (HRTEM) image clearly shows the crystalline nature of the UNCs (Figure S2c). The UV−vis absorption spectrum (Figure 1f; also see the additional discussion in the SI) implies that the sizes of the UNCs are in the quantum-confinement range. Characterizations by X-ray diffraction (XRD) and photoluminescence (PL) spectroscopy are given in Figures S4 and S5, respectively.

For ultrathin nanocrystals, the surface energy is high because of the large surface-to-volume ratio, which makes a dominant

Received: March 27, 2013
Published: April 23, 2013

 © 2013 American Chemical Society dx.doi.org/10.1021/ja403065z | J. Am. Chem. Soc. 2013, 135, 6834−6837

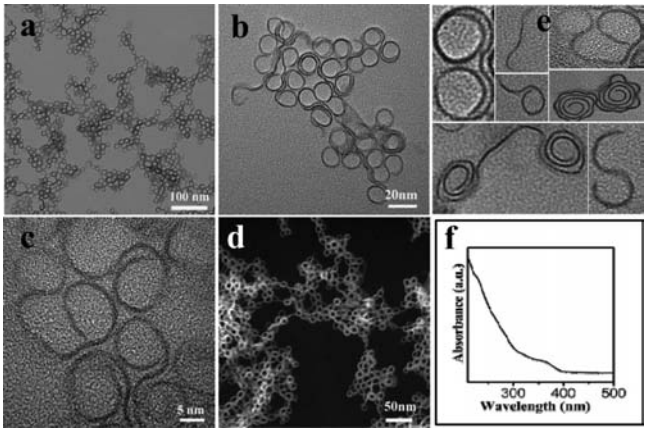

Figure 1. (a, b) Typical TEM images, (c) HRTEM image, and (d) STEM image of the as-synthesized UNCs. (e) Images showing versatile shapes of UNCs with different coiling levels of nanoribbons. (f) UV−vis spectrum of UNCs.

contribution to the total energy of the system. From the viewpoint of energetics, if the energy of bending a ribbon into a coil ($|E_b|$) is larger than the strain energy resulting from the induced curvature (E_s), the formation of coils would be favorable. E_b involves the surface energy of the ultrathin nanoribbons and the energy stabilization due to attractive ligand−ligand interactions resulting from overlapping (interdigitation) of ligands on the coil surface. From a simple beam model based on continuum mechanics, the strain energy can be expressed as[27] $E_s = YIl/2R^2$, where Y is the Young modulus, $I = bh^3/12$ is the geometrical moment of inertia of a nanoribbon having a width b and a thickness h, l is the contour length of the nanocoil, and R is the radius of the resulting coil. The quantity YI presents the flexural rigidity, which is strongly dependent on the ribbon thickness h through the factor h^3. In other words, the thinner the ribbon, the more flexible it will be. Thus, the structural flexibility of the UNCs here derives from the subnanometer-scale thickness of the nanoribbons. As E_s is inversely proportional to the square of R, higher strain energy is stored when forming coils with a smaller radius R, and consequently, bending with high curvature becomes unfavorable. The radii of the nanocoils in final state are similar (Figure 1), resulting from the energy equilibrium between the opposing quantities E_b and E_s. A TEM image of the sample obtained after a short reaction time (Figure S6) shows amorphous aggregates with bent strips, suggesting that the growth of ultrathin nanoribbons from solution occurs in association and concurrent with the self-coiling. In addition, strain present in both sides of the nanoribbon usually stimulates bending or rolling. If the two sides of the ribbon are not equal, a strain will be created that will stimulate coiling toward one direction. However, we observed that the coiling direction of the ribbon was random (Figure 1e). Alternatively, the fact that the near-molecular diameter and high aspect ratio of the ultrathin nanoribbons approach those of linear polymer molecules allows the ultrathin nanoribbons in solution to be similarly viewed as semiflexible polymers, which are often modeled as wormlike polymer chains using statistical mechanics. Sano et al.[23] modeled the ring formation of single-walled carbon nanotubes (SWNTs) by treating the SWNTs as wormlike polymer chains and found that thermal fluctuation can bend a SWNT if its length exceeds the Kuhn segment length. From our results, the geometry of the nanoribbons is comparable with that of SWNTs, making a similar case possible. The UNCs are formed under solvothermal conditions, where the thermal fluctuations in solvent molecules are strong and likely significant for the formation of UNCs with various conformations. Meanwhile, surface-adsorption-induced strain and solvent effects may make the coiling more favorable.

The alkylamine in the synthetic system plays an important role in the formation of the UNCs, not only serving as both the solvent and capping ligand but also providing an additional stabilization, if any, resulting from the ligand−ligand interactions on the curved surface. To exploit the effects, we performed control experiments under identical experimental conditions but using amines with different alkyl-chain lengths. We found that dodecylamine could produce similar nanocoils as those observed in the case of octylamine. However, neither oleylamine nor butylamine produced good-quality nanocoils, although trace quantities of nanocoils could be observed (Figure S7). This may indicate that there exists an optimal interaction between the organic ligands for the formation of UNCs. If the alkyl chains are too long, they may introduce steric repulsion that counterbalances the attractive interactions on the coil surface; if the alkyl chains are too short, the attractive interactions among neighboring ligands upon coiling may be too weak. Both cases are unfavorable for the formation of UNCs.

It is worth noting that these UNCs have a tendency to self-organize into superlattices during the synthesis. This was more obvious when the content of ethanol in the system was reduced and occurred even in the absence of ethanol. A typical few-layered assembly of UNCs was revealed by TEM (Figure 2;

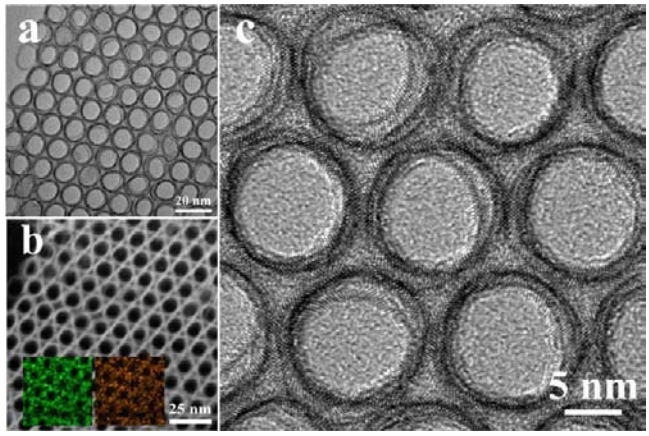

Figure 2. (a) TEM and (b) STEM images of a typical superlattice self-assembled from UNCs with two-dimensional hexagonal packing. The insets in (b) are EDX elemental maps, which clearly indicate that indium and sulfur are uniformly distributed in the UNCs. (c) HRTEM image of the UNC superlattice. The crystal lattices of the coils clearly suggest that the framework of the assembly structure is composed of crystalline inorganic components.

enlarged images are shown in Figure S8). It seems that the UNCs can self-adjust their flexible conformations more tightly to form ordered regions. Although isolated UNCs possess flexible coil conformations, those nanocoils in the superlattices all take uniform circular morphologies with a diameter of ~13 nm. The UNC superlattice looks more like an ordered two-dimensional porous structure with uniform pore features. The scanning TEM (STEM) image shows more clearly the uniform frameworks composed of nanocoils (Figure 2b). Energy-dispersive X-ray (EDX) mapping analysis confirmed the even distribution of indium and sulfur along the framework of the assembly structure (Figure 2b insets). A typical HRTEM image shows bending

dx.doi.org/10.1021/ja403065z | J. Am. Chem. Soc. 2013, 135, 6834−6837

lattices along the loops, further indicating that the "porous" superlattice is composed of crystalline inorganic materials (Figures 2c and S8c). In the superlattice structure, we can also see double-headed S-shaped coils with tight loops and uniform head coils. This further suggests that when forming assemblies, the nanocoils self-adjust their shapes to crystallize because of the morphology flexibility resulting from their ultrathin nanostructures.

Prolonging the synthesis time to several days and reducing the content of ethanol in the system (for details, see the SI) afforded three-dimensional self-assemblies of UNCs. After the reaction was complete, the precipitate was washed with ethanol cautiously to avoid destroying the assembled crystals. Although many isolated UNCs still existed, this reaction yielded numbers of relatively large UNC crystals with sizes of more than 500 nm that were composed of thousands of UNCs (Figures 3 and S9). A

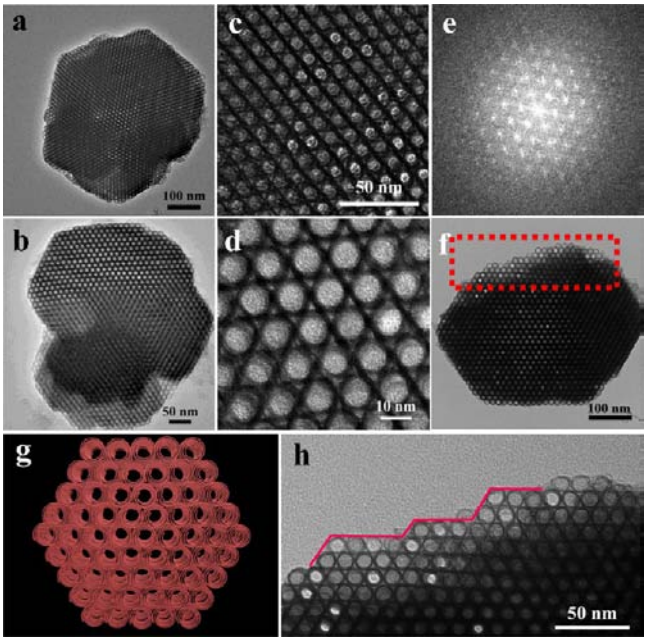

Figure 3. (a, b) TEM images of nanocoil supercrystals with a size of ~500 nm. (c, d) Enlarged TEM images of the supercrystals in the left column, clearly showing the regular inner structure. (e) FFT pattern of the supercrystal in (a). (f) TEM image of a supercrystal showing an "unsmooth" surface. (g) Schematic model of a supercrystal. (h) Enlarged view of the red rectangle in (f).

series of TEM images of incomplete superlattices indirectly reveal the growth process from isolated UNCs to UNC superstructures (Figure S10). In this case, more UNCs with different conformations packed together and self-adjusted their conformations to adapt to a change in the assembly system, and thus, the building units in the superstructures appeared as uniform "pores" (Figure 4). This process is somewhat similar to the crystallization of macromolecules, in which their molecular chains fold into well-behaved structures and form ordered regions by interactions between molecular chains. These nanocoil supercrystals possess regular arrays of uniform large pores (13 nm in diameter), very similar to typical ordered mesoporous structures in appearance. The supercrystals are highly ordered, as evidenced by the fast Fourier transform (FFT) pattern (Figure 3e). In fact, the nanocoils are assembled into arrays in which the ultrathin nanocoils themselves act as inorganic walls, thus spontaneously forming pores. The best

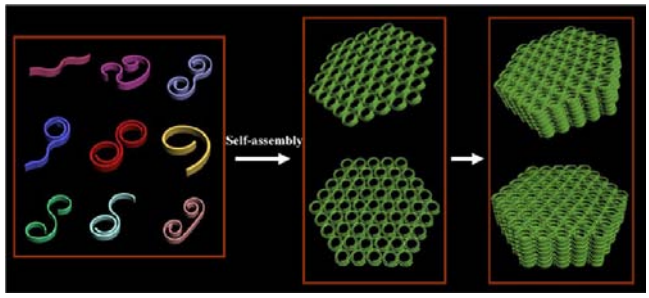

Figure 4. Scheme for the formation of supercrystals from isolated nanocoils with flexible shapes.

images were obtained when the assembled structure was thin, showing clearly the regular inner structures (Figure 3c,d). Interestingly, some crystals exposed rough edge surfaces in which the nanocoils' arrangement, like atoms, showed steps that are usually observed in high-index faceted nanocrystals (Figure 3f,h). Examination of different time points of samples obtained under same synthetic conditions by TEM revealed a size evolution of UNC supercrystals. Although no linear correlation between size and time was found, the supercrystals underwent a gradual growth stage with increasing time. The size of UNC superstructures reached up to 1−2 μm in 60 h (Figure S11).

For the formation of supercrystals, ultrathin structures and high aspect ratios enable the UNCs to be flexible in conformation, and therefore, random nanocoils can self-adjust their shapes to be more compact and form supercrystals in order to minimize the total surface free energy of the system. Additionally, the flexibility of these "soft" UNCs allows themselves to overlap and interweave with each other; in this way, the superstructures can be stabilized. It is known that the capping ligands on the nanocrystal dominate the interparticle interactions, structure, and cohesion of the nanocrystal superlattice.[28] For the UNC supercrystals, the interactions are also influenced by the alkylamine on the nanocoil surfaces. An HRTEM image of the superlattice (Figure 2c) shows overlaps and "bonds" among neighboring nanocoils, which are also observed in the frameworks of three-dimensional supercrystals (Figure 3). These facts suggest there are strong interactions between nanocoils in the assembled structures, likely through bundling and interdigitation of surface ligands, which provide stacking energy and make the formation of supercrystals more favorable.

When the UNCs precipitated in ethanol were incubated for several days, they gradually gave transparent crystal-like macroscopic solids with sizes of up to 1−3 mm. A typical sample was observed using optical instruments (Figure 5). Polarizing microscopy is most commonly used to view minerals, biopolymers, liquid crystals, and so on; birefringence is often observed in materials with anisotropic crystal structures.[29,30] Here we observed strong birefringence in some domains of the macrostructures under cross-polarized illumination (Figures 5b and S12), implying some regularities in the internal arrangement of the constituents present in the structures. In view of the fact that the UNCs have the tendency to form superlattices and supercrystals, it is not surprising that these macrostructures formed. As a result of the optical properties of the building units (Figure S5b), red and green fluorescence images of the macroscopic assembly were obtained using PL microscopy under different excitation and emission filters, respectively (Figure 5c,d).

dx.doi.org/10.1021/ja403065z | J. Am. Chem. Soc. 2013, 135, 6834−6837

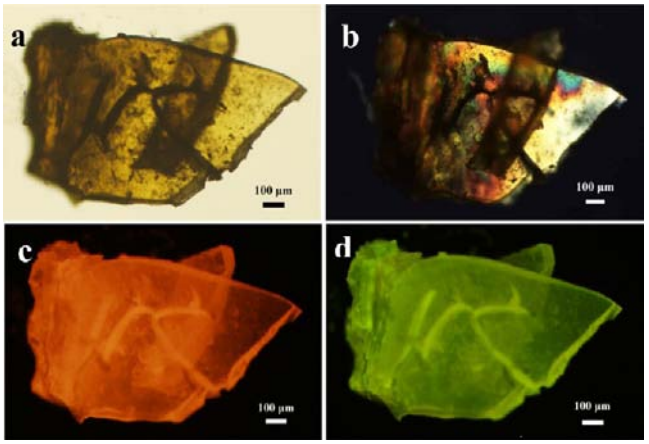

Figure 5. (a) Optical micrograph of an assembled nanocoil aggregate formed in the nanocoil solution after about 2 weeks. (b) Cross-polarized micrograph of the sample in (a) showing significant birefringence. (c, d) Fluorescence micrographs obtained using an Olympus IX70 microscope.

Self-assembly of inorganic nanocrystals usually requires a controlled size distribution in order to get uniform rigid building units. In contrast, the UNCs presented here possess relatively flexible one-dimensional shapes and can self-adjust their shapes and assemble into superstructures, which is similar to the folding and crystallization process of biomacromolecules. Moreover, the formation of UNC supercrystals will be of great interest not only for providing insights into the self-assembly of ultrathin one-dimensional nanostructures but also for understanding the fundamental crystallization of flexible polymers. We hope our study presents a potentially ideal platform for bringing closer the domains of inorganic colloids and organic macromolecules.

■ ASSOCIATED CONTENT

Supporting Information

Synthesis details, TEM images, FTIR spectra, and other characterization data. This material is available free of charge via the Internet at http://pubs.acs.org.

■ AUTHOR INFORMATION

Corresponding Author

wangxun@mail.tsinghua.edu.cn

Notes

The authors declare no competing financial interest.

■ ACKNOWLEDGMENTS

This work was supported by the National Natural Science Foundation of China (91127040 and 21221062) and the State Key Project of Fundamental Research for Nanoscience and Nanotechnology (2011CB932402).

■ REFERENCES

(1) Henzie, J.; Grunwald, M.; Widmer-Cooper, A.; Geissler, P. L.; Yang, P. *Nat. Mater.* **2012**, *11*, 131.
(2) Wang, T.; Zhuang, J.; Lynch, J.; Chen, O.; Wang, Z.; Wang, X.; LaMontagne, D.; Wu, H.; Wang, Z.; Cao, Y. C. *Science* **2012**, *338*, 358.
(3) Sun, Z.; Bai, F.; Wu, H.; Schmitt, S. K.; Boye, D. M.; Fan, H. *J. Am. Chem. Soc.* **2009**, *131*, 13594.
(4) Chen, Q.; Bae, S. C.; Granick, S. *Nature* **2011**, *469*, 381.
(5) Li, F.; Josephson, D. P.; Stein, A. *Angew. Chem., Int. Ed.* **2011**, *50*, 360.
(6) Fan, H.; Yang, K.; Boye, D. M.; Sigmon, T.; Malloy, K. J.; Xu, H.; Lopez, G. P.; Brinker, C. J. *Science* **2004**, *304*, 567.
(7) Xia, Y.; Nguyen, T. D.; Yang, M.; Lee, B.; Santos, A.; Podsiadlo, P.; Tang, Z. Y.; Glotzer, S. C.; Kotov, N. A. *Nat. Nantechnol.* **2011**, *6*, 580.
(8) Glotzer, S. C.; Solomon, M. J. *Nat. Mater.* **2007**, *6*, 557.
(9) Bishop, K. J.; Wilmer, C. E.; Soh, S.; Grzybowski, B. A. *Small* **2009**, *5*, 1600.
(10) Heim, M.; Romer, L.; Scheibel, T. *Chem. Soc. Rev.* **2010**, *39*, 156.
(11) Marth, J. D. *Nat. Cell Biol.* **2008**, *10*, 1015.
(12) Smith, L. J.; Fiebig, K. M.; Schwalbe, H.; Dobson, C. M. *Folding Des.* **1996**, *1*, R95.
(13) Lindorff-Larsen, K.; Røgen, P.; Paci, E.; Vendruscolo, M.; Dobson, C. M. *Trends Biochem. Sci.* **2005**, *30*, 13.
(14) de la Torre, J. G.; Cifre, J. G. H.; Martinez, C. L. P. *Eur. J. Phys.* **2008**, *29*, 945.
(15) Flory, P. J. *Statistical Mechanics of Chain Molecules*; Oxford University Press: New York, 1989.
(16) Huo, Z.; Tsung, C.; Huang, W.; Zhang, X.; Yang, P. *Nano Lett.* **2008**, *8*, 2041.
(17) Korgel, B. A. *Science* **2004**, *303*, 1308.
(18) Pan, Z. W.; Dai, Z. R.; Wang, Z. L. *Science* **2001**, *291*, 1947.
(19) Cademartiri, L.; Guerin, G.; Bishop, K. J. M.; Winnik, M. A.; Ozin, G. A. *J. Am. Chem. Soc.* **2012**, *134*, 9327.
(20) Chen, L.; Wang, H.; Xu, J.; Shen, X.; Yao, L.; Zhu, L.; Zeng, Z.; Zhang, H.; Chen, H. *J. Am. Chem. Soc.* **2011**, *133*, 9654.
(21) Kong, X. Y.; Ding, Y.; Yang, R.; Wang, Z. L. *Science* **2004**, *303*, 1348.
(22) Gao, P. X.; Ding, Y.; Mai, W.; Hughes, W. L.; Lao, C.; Wang, Z. L. *Science* **2005**, *309*, 1700.
(23) Sano, M.; Kamino, A.; Okamura, J.; Shinkai, S. R. *Science* **2001**, *293*, 1299.
(24) Martel, R.; Shea, H. R.; Avouris, P. *Nature* **1999**, *398*, 299.
(25) Xu, X.; Zhuang, J.; Wang, X. *J. Am. Chem. Soc.* **2008**, *130*, 12527.
(26) Kotov, N. A. *Science* **2010**, *330*, 188.
(27) Martel, R.; Shea, H. R.; Avouris, P. *J. Phys. Chem. B* **1999**, *103*, 7551.
(28) Wang, Z. L.; Harfenist, S. A.; Whetten, R. L.; Bentley, J.; Evans, N. D. B. *J. Phys. Chem. B* **1998**, *102*, 3068.
(29) Taden, A.; Landfester, K.; Antonietti, M. *Langmuir* **2004**, *20*, 957.
(30) Du, C.; Falini, G.; Fermani, S.; Abbott, C.; Moradian-Oldak, J. *Science* **2005**, *307*, 1450.